



Research

Cite this article: Westerling ALR. 2016

Increasing western US forest wildfire activity: sensitivity to changes in the timing of spring.

Phil. Trans. R. Soc. B **371**: 20150178.

<http://dx.doi.org/10.1098/rstb.2015.0178>

Accepted: 23 March 2016

One contribution of 24 to a discussion meeting issue 'The interaction of fire and mankind'.

Subject Areas:

environmental science

Keywords:

wildfire, climate, forest

Author for correspondence:

Anthony LeRoy Westerling

e-mail: leroy.westerling@icloud.com

Increasing western US forest wildfire activity: sensitivity to changes in the timing of spring

Anthony LeRoy Westerling

Sierra Nevada Research Institute, University of California, Merced, 5200 N. Lake Road, Merced, CA 95343, USA

ALW, 0000-0003-4573-0595

Prior work shows western US forest wildfire activity increased abruptly in the mid-1980s. Large forest wildfires and areas burned in them have continued to increase over recent decades, with most of the increase in lightning-ignited fires. Northern US Rockies forests dominated early increases in wildfire activity, and still contributed 50% of the increase in large fires over the last decade. However, the percentage growth in wildfire activity in Pacific northwestern and southwestern US forests has rapidly increased over the last two decades. Wildfire numbers and burned area are also increasing in non-forest vegetation types. Wildfire activity appears strongly associated with warming and earlier spring snowmelt. Analysis of the drivers of forest wildfire sensitivity to changes in the timing of spring demonstrates that forests at elevations where the historical mean snow-free season ranged between two and four months, with relatively high cumulative warm-season actual evapotranspiration, have been most affected. Increases in large wildfires associated with earlier spring snowmelt scale exponentially with changes in moisture deficit, and moisture deficit changes can explain most of the spatial variability in forest wildfire regime response to the timing of spring.

This article is part of the themed issue 'The interaction of fire and mankind'.

1. Introduction

Beginning in the mid-1980s, forest wildfire activity in western US forests underwent an abrupt and sustained regional increase, with nearly two-thirds of that increase concentrated in forests of the Northern US Rocky Mountains between 42° and 50° N latitude [1]. This change in Northern US Rocky Mountain forest wildfire has been linked to climatic factors such as warmer temperatures, dry summers, below-average winter precipitation or earlier spring snowmelt [1–4]. Analyses of reconstructed paleo wildfire and climate indices have also shown similar associations between widespread Northern US Rockies fire years and warm springs combined with warm and dry summers [5,6]. Warming temperatures increase vapour pressure deficit and evapotranspiration, with effects on wildfire, other disturbance and mortality, and forest productivity [7].

The timing, extent and severity of wildfire in western US forests is strongly influenced by climate: over seasonal to decadal time scales antecedent climate shapes fuel characteristics such as their amount, connectivity and structure, while seasonal to interannual climate variability governs fuel flammability [8–10]. A changing climate consequently alters forest fuels characteristics across multiple time horizons. Species compositions and productivity may change as higher temperatures affect potential growing-season length and changes in precipitation, and temperature-driven changes in evapotranspiration affect the moisture available for growth [8,9]. Flammability may be altered as changing evapotranspiration and precipitation affect the moisture available for wetting fuels. Dynamic interactions between wildfire (as well as other disturbance types) that kill standing trees, and altered climatic conditions for

subsequent germination, recruitment and growth of new vegetation, have the potential to produce abrupt, nonlinear transformations of the landscape in response to incremental climate changes [11].

Most of the western US is arid with a preponderance of annual precipitation coming in winter [12]. Much of the forest area is concentrated in mountain ranges where orographic effects enhance precipitation amount, and the elevation increases the likelihood for winter precipitation to fall as snow that can accumulate and carry moisture from cool season precipitation into the more arid summer [12]. Projections of future climate in the region indicate a potential for significant trends toward drier conditions and a reduced fraction of precipitation coming as snow [13,14]. Consequently, it is natural to hypothesize that an early consequence of a warming climate might be a rapid acceleration of wildfire activity in forests at elevations where snow plays an important role in the hydrology, but the climate is warm enough that a modest temperature increase could significantly shift the timing of the spring snowmelt. In 2006, Westerling *et al.* [1] found early indications that this might well be the case, attributing a majority of the regional increase in large forest fire frequency through 2003 to fires burning primarily in mid-elevation Northern US Rocky Mountains forests in early snowmelt years.

The work presented here seeks to answer several questions: has forest wildfire activity across the region continued to increase? Are there new 'hot spots' of increasing fire activity in the region's forests as temperatures have continued to increase? Has recent wildfire activity been associated with the same patterns of temperature and spring snowmelt timing? Can we explain spatial variation in the response of wildfire activity to recent climate trends within the regions' forests? Is fire activity changing in other vegetation types, and if so, is it also associated with the timing of spring snowmelt?

To address these questions, we update the 2006 analysis of Westerling *et al.* [1], extend it to consider the spatial variation in wildfire response to the timing of spring within western US forests, and take a preliminary look at wildfire trends in non-forest vegetation.

2. Data and methods

(a) Fire history

Fire histories for the US National Park Service (NPS), Bureau of Indian Affairs (BIA) and Bureau of Land Management (BLM) were obtained from the US Department of Interior (http://fam.nwcg.gov/fam-web/weatherfirecd/fire_files.htm) and for the US Forest Service (USFS) from the US Department of Agriculture (<http://fam.nwcg.gov/fam-web/kcfast/mnmenu.htm>), and used to update and extend Westerling *et al.*'s fire history [1,4]. We use the same methodology here to create a comprehensive history of actively suppressed wildfires greater than 400 ha reported burning in all vegetation types by USFS, NPS and BIA for 1970–2012, as well as by BLM for 1980 through 2012. USFS, NPS and BIA manage over 70% of the forest area in the western United States, and more than 80% of the forest area over 1370 m elevation (estimates derived from the federal lands and forest area datasets described below). BLM manages mostly rangelands, as well as an additional approximately

4% of western US forest area, and while shorter, the available record allows for more spatially comprehensive comparisons across wildfires in different vegetation types.

About 99% of recorded fires in our dataset are less than 400 ha in size, but comprise only about 25% of total burned area. Documentary records for less than 400 ha fires frequently have missing data fields and erroneous or incomplete location data. Fires greater than 400 ha comprise most burned area, while the smaller number of records facilitates quality assurance; larger fires also usually have better data quality (probably because their costs bring greater scrutiny) [1]. A small number of extremely large wildfires dominate the burned-area record, and multiple management entities often produce conflicting, duplicate records for suppression on the same fire. Fire records were compared using simple algorithms linking date, name, approximate size and location, and obvious duplications and errors were corrected [1,4]. Individual records corresponding to very large fires and fire complexes were compared with archived daily situation reports from the National Interagency Fire Center (<http://www.nifc.gov>), diverse media reports, and post-fire rehabilitation studies to help identify duplications and errors in the records, with particular attention to size and vegetation types.

(b) Land surface characteristics and forest masks

Gridded topographic information derived from the GTOPO30 Global 30 Arc Second (approx. 1 km) Elevation Dataset (elevation, slope, aspect) and coarse vegetation types using the University of Maryland vegetation classification scheme were accessed online from the North American Land Data Assimilation System (LDAS) (<http://ldas.gsfc.nasa.gov>) [15]. These data were combined with GIS layers of federal and tribal land ownership (accessed online from the US National Atlas http://nationalmap.gov/small_scale/atlasftp.html) using spatial packages in R (<https://cran.r-project.org>) to create masks of federal ownership, and gridded elevation and forest fraction for the western US on a 1/8 degree longitude/latitude grid. Masks for six western US forest areas managed collectively by BIA, NPS and USFS were created based on the methodology in [1] for: the Northern Rockies between 42° and 49° N latitude (NR); the Southern Rockies below 42° N (SR); mountain ranges of Arizona and New Mexico excluding the Southern Rockies (SW); the mountains of coastal southern and central California (SC); the Sierra Nevada and southern Cascades and Coast Ranges (SN); and the Cascades and Coast Ranges above 43.1° N (NW). SC fires burning predominantly forest vegetation were very few, with no statistically significant trends detectable. The largest SC wildfires tend to be wind-driven autumn fires that primarily burn in chaparral, but which can also burn significant forest area. Consequently, the small SC forest area is excluded in most subsequent analyses.

(c) Gridded hydroclimatic records

Gridded daily climate data derived from historical station observations using the index station method [16] for 1915–2012 were obtained from the University of Washington National Hydrologic Prediction System (NHPS) (<http://www.hydro.washington.edu/forecast/westwide/>). NHPS data did not incorporate all potentially available stations but were updated monthly, providing up-to-date time series using stations with high-quality records. We also

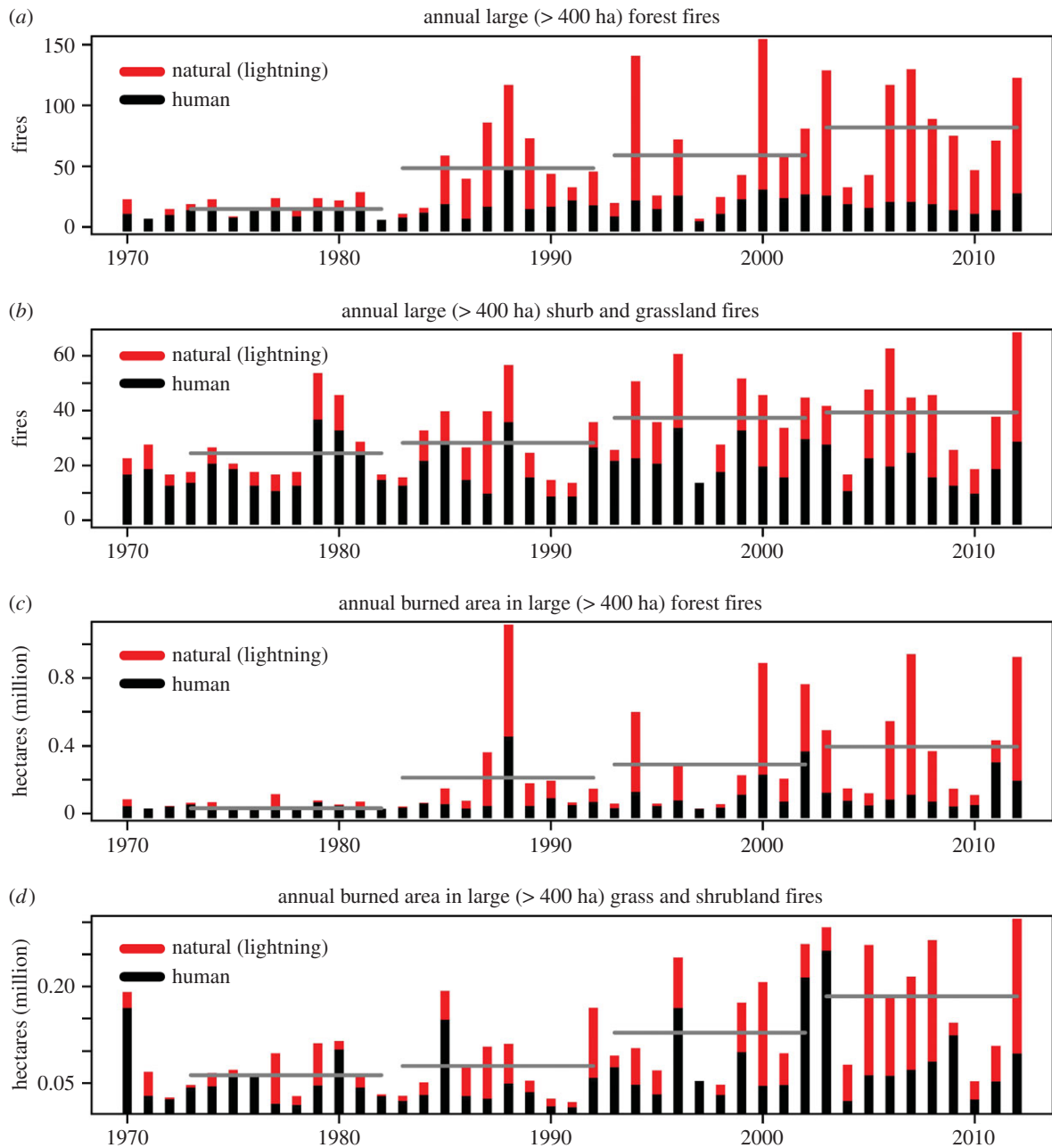


Figure 1. Human and lightning-ignited annual large forest fires, (a), grass and shrubland fires (b), forest burned area (c), and grass and shrub burned area (d), on Forest Service, Park Service and Indian Lands in the western US. Horizontal lines indicate decadal averages.

obtained from NHPS actual evapotranspiration (AET) and snow-water equivalent (SWE) simulated with the variable infiltration capacity (VIC) hydrologic model [17] at a daily time step in water balance mode forced with the daily climate data, LDAS vegetation and topography, and climatological winds. Potential evapotranspiration (PET) was estimated using the Penman–Montieth equation with the same forcing data, and used with AET to calculate moisture deficit ($D = PET - AET$) [1,18,19]. D was then aggregated to monthly cumulative values.

(d) Trend analysis of wildfire frequency and burned area by coarse vegetation type

Number and burned area of large forest wildfires on BIA, NPS and USFS lands were aggregated annually by coarse vegetation type ('forest' versus 'non-forest') derived from documentary fire history data. Annual large-fire frequency

and burned area time series were plotted by coarse vegetation type and reported ignition source (human- versus lightning-caused ignitions; figure 1). Decadal averages were calculated (figure 1) and pairwise comparisons using two-sided Mann–Whitney [20] tests of the null hypothesis that each subsequent decade's fire frequency and burned area distributions have the same mean as for 1973–1982 (tables 1–2). Trends were fit to annual burned area time series for forest and non-forest fires using linear regression techniques with the $\text{glm}()$ function in R.

(e) Generalized Pareto log-fire size distributions

Generalized Pareto distributions (GPDs) [21] characterize the distribution of exceedances over a threshold. Here we binned individual fire records in the combined BIA, NPS USFS fire history by decade and coarse vegetation type, and fit GPDs to the logarithm of fire sizes exceeding a 400 ha threshold

Table 1. Per cent change in wildfires over 1973–1982 average.^a

| | 1983–1992 | 1993–2002 | 2003–2012 |
|-------------------|---------------|---------------|----------------|
| five forest areas | +259% (0.014) | +361% (0.013) | +556% (<0.001) |
| Northern Rockies | +532% (0.006) | +589% (0.087) | +889% (<0.001) |
| Northwest | +200% (0.046) | +514% (0.050) | +1000% (0.001) |
| Sierra Nevada | +219% (0.094) | +184% (0.110) | +274% (0.008) |
| Southwest | +71% (0.618) | +221% (0.040) | +462% (<0.001) |
| Southern Rockies | –6% (0.449) | +306% (0.180) | +256% (<0.001) |

^a*p*-values for two-sided Mann–Whitney test in parentheses.

Table 2. Per cent change in burnt area over 1973–1982 average.^a

| | 1983–1992 | 1993–2002 | 2003–2012 |
|-------------------|----------------|----------------|-----------------|
| five forest areas | +640% (0.015) | +911% (0.035) | +1271% (<0.001) |
| Northern Rockies | +2093% (0.005) | +1784% (0.104) | +2966% (0.002) |
| Northwest | +428% (0.034) | +2149% (0.061) | +4979% (0.001) |
| Sierra Nevada | +270% (0.307) | +492% (0.161) | +324% (0.011) |
| Southwest | +42% (0.791) | +668% (0.046) | +1266% (0.004) |
| Southern Rockies | –31% (0.405) | +659% (0.054) | +331% (0.002) |

^a*p*-values for two-sided Mann–Whitney test in parentheses.

using the `gpd.fit()` maximum-likelihood fitting function in the `ismev` library in R (figure 2).

(f) Regional spring and summer temperature index

Consistent with [1], a regional spring and summer temperature index was derived from temperature data accessed from the National Oceanic and Atmospheric Administration Drd964x Climate Division temperature dataset ([22]; <ftp://ftp.ncdc.noaa.gov/pub/data/cirs/drd/divisional.README>). Mean monthly temperature values (1970–2012) for 110 western US Climate Divisions for March through August of each year were averaged to produce an annual regional index of spring and summer temperature, which was compared with the annual large forest fire frequency on BIA, NPS and USFS lands (figure 3).

(g) Snowmelt timing

For the timing of the spring snowmelt 1970–2002, Westerling *et al.* [1] used the first principal component of the dates of the centre of mass of annual flow (CT1) for 240 snowmelt-dominated streamflow gauge records provided by the US Geological Survey (USGS) Hydro-Climatic Data Network and by Environment Canada [23–25]. We updated this index for 1970–2012, using a subset of stations provided by USGS. Both Westerling *et al.*'s [1] index and our updated reconstruction are presented here for comparison (figure 3). Missing values for each station were replaced with the 1970–2002 mean for that station. CT1 accounts for one-fifth of total variance in CT and is essentially the annual average CT value for western US stations, with a coherent regional signal in snowmelt timing [1]. The 14 earliest and latest

snowmelt years were extracted from the 1973–2012 record portion for comparison of wildfire and climate covariability with spring snowmelt timing (figure 3).

(h) Fire season length and fire burn time

Documentary wildfire discovery dates and control dates were converted to Julian day of the year using the `julian()` function in R (<https://cran.r-project.org>). The time between first discovery and last control of a large fire in each year was used to proxy for fire season length [1] (figure 3). The time between discovery and control for each large fire is assumed to be indicative of the period of its active spread, when wildfire activity is probably affected by climatological and meteorological factors.

(i) Snowmelt timing tercile analysis of burned area by coarse vegetation type

For a tercile analysis of burned area, wildfire area burned was summed to produce total annual burned area by year and coarse vegetation type (forest or non-forest)—using discovery year and fire type from the documentary fire history—for the common 1973–2012 record from the combined USFS, NPS and BIA fire histories, and for the 1980–2012 record for BLM. Box and whisker plots of annual burned area time series sub-setted by snowmelt timing tercile, coarse vegetation type and fire history were created in R using the `boxplot()` function. Sub-setted time series were compared using the Kruskal–Wallis rank sum test of the null hypothesis that the location parameters of all the sub-setted time series were the same, and multiple pairwise comparisons

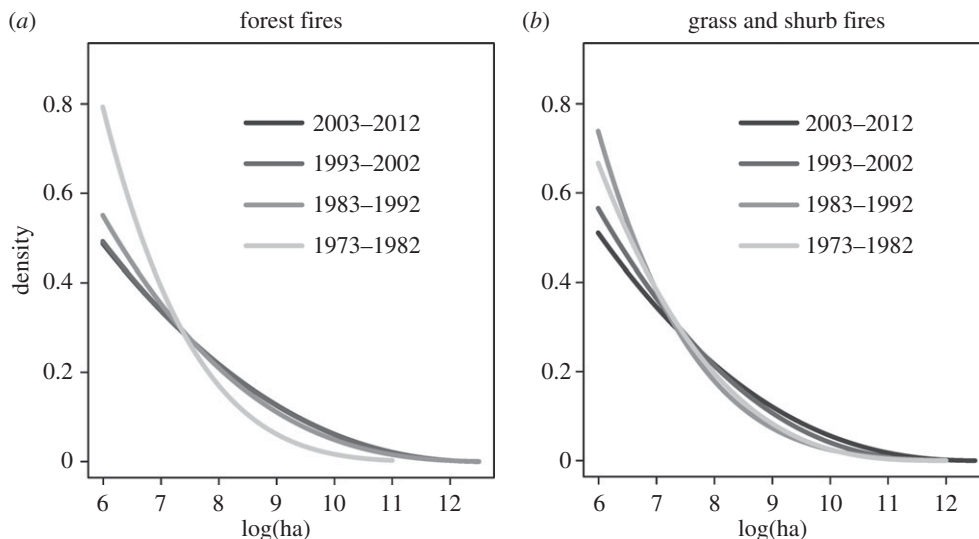


Figure 2. Generalized Pareto distributions fit to log(fire size), by decade for forest fires (a), and grass and shrub fires (b).

using Dunn's z-test statistic for pairwise differences in median using `dunn.test` package in R [26].

(j) Gridded forest-area weighted moisture deficit

Gridded forest-area weighted moisture deficit ($A\delta$) integrates both the intensity of drying and the forest area affected by drying associated with a shift from late to early springs. $A\delta$ was calculated for 300 m elevation bands in each gridded forest area (figure 5) as follows:

$$A\delta_{F,E} = \sum_{g(F,E)} a\delta_g, \text{ where } \delta = \frac{D^{\text{early}} - D^{\text{late}}}{D^{\text{early}} + D^{\text{late}}}$$

a = fraction of grid cell in forest vegetation; D^{early} = average of 14 early snowmelt years' cumulative water year moisture deficit; D^{late} = average of 14 late snowmelt years' cumulative water year moisture deficit; F = Forest {NW, NR, SN, SR, SC, SW}; E = Elevation in 300 m (1000 ft) bands, $g(F, E)$ = 1/8 degree longitude \times latitude grid cells per forest and elevation band.

Elevation bands in each forest area for which the summed forest fractions in aggregate comprised less than one 1/8 degree grid cell in area were excluded from analysis. Forest areas in grid cells above 2895 m were also excluded from analysis, as a rough proxy for the regional upper treeline elevation.

(k) Determinants of cumulative forest-area weighted moisture deficit sensitivity to snowmelt timing

Average monthly SWE was derived from daily cumulative SWE simulated by VIC on a 1/8 degree grid, and intersected with the forest masks and elevation in R to produce a time series of monthly average SWE for the grid cells in each forest area and elevation band. Monthly average SWE < 1 mm was defined as 'snow-free' conditions. Over the grid cells in each combination of forest area and elevation band, the mean snow-free season length in months (SFI) was calculated for 1950–1999. Similarly, the average April through August cumulative AET was calculated over the same period for each forest area and elevation band. A scatter plot with point areas scaled to represent the forest-area weighted change in deficit ($A\delta_{F,E}$) for each forest (F) and elevation band (E) was plotted over mean SFI and mean

April–August cumulative AET (figure 5), to show how drying due to changes in snowmelt timing is a function of the length of the snow-free season and moisture limits on evapotranspiration in late spring and summer.

(l) Comparison of fire frequency to cumulative forest-area weighted moisture deficit

The aggregate number of large wildfires for 14 early and 14 late snowmelt years was calculated by forest and elevation as follows. Large wildfire locations were gridded to the nearest centroids of the 1/8 degree grid used here for analysis, and intersected with gridded masks for each of the six forest areas. Because of imprecision in documentary fire locations, large wildfires located within one 1/8 degree grid cell of a forest area were included in the total for that forest area. Elevations were derived from the documentary record for each wildfire, rather than the nearest 1/8 degree grid cell. For each forest area and elevation band, the number of large wildfires was summed by intersecting wildfire discovery year with years of early or late spring snowmelt. The difference between the early and late snowmelt year wildfire totals was graphed for each forest and elevation band versus the corresponding $A\delta_{F,E}$ (figure 5), and a diverse array of linear and nonlinear regression model functional forms were fitted in R using the `glm()` function. The model selected to describe the relationship between changes in wildfire frequency and changes in forest-area weighted moisture deficit related to a shift in the timing of spring had the best Akaike Information Criterion [27] combined with the best visual fit to the data and high R^2 value.

3. Results

(a) Trends in large-fire frequency and burned area

Our update on the Westerling *et al.* [1] analysis finds that the frequency of large forest wildfires has continued to increase, with each decade since the 1970s, showing an increased frequency of large wildfires at a regional scale compared with preceding decades (figure 1, table 1). We find a highly significant trend ($p < 0.0001$) over 1973–2012, equivalent to over 20 additional large fires per decade on USFS, NPS and BIA

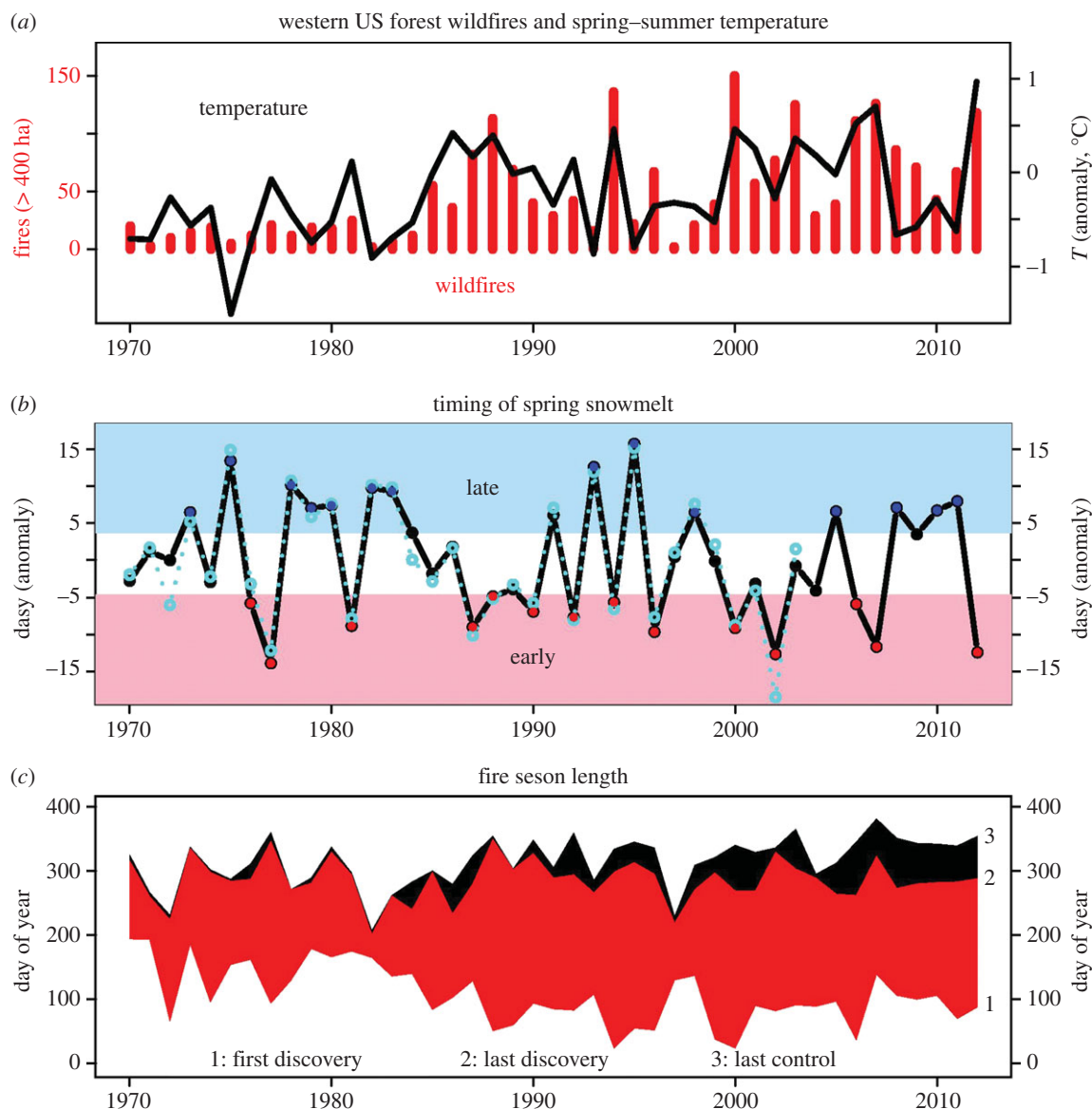


Figure 3. (a) Annual frequency of large (> 400 ha) western US forest wildfires (bars) and mean March through August temperature for the western US (line). Spearman's rank correlation between the two series is 0.69 ($p < 0.001$). (b) First principle component of centre timing of streamflow in snowmelt-dominated streams from Westerling *et al.* [1] (dashed line), and updated through 2012 (solid line). Low (pink shading), middle (no shading) and high (light blue shading) tercile values indicate early, mid- and late timing of spring snowmelt, respectively. (c) Annual time between first and last large-fire discovery and last large-fire control. This figure is an updated version of a previously published figure [1].

lands, or more than 140% of the annual average for the first decade of forest fires (not shown). The area burned in these large fires has also continued to increase (figure 1, table 2), with both a shift in the fire size distribution for fires exceeding 400 ha that was particularly pronounced in the 1980s (figure 2), and the ongoing increase in large wildfire frequency contributing to the overall increase in forest wildfire burned area. The fitted linear trend in forest wildfire burned area was also highly significant ($p = 0.002$, figure 2), equivalent to 123 000 ha per decade since the 1970s, or increasing on average by nearly 390% of the annual average for the first decade in each subsequent decade.

In addition, we find significant increases in wildfire activity in non-forest vegetation types within the same federal land management units (figure 1). The trend in the frequency of large non-forest wildfires is statistically significant ($p = 0.009$), and the trend in the area burned in these large non-forest wildfires is highly significant ($p = 0.0001$),

equivalent to 40 585 ha per decade since the 1970s, or 65% of annual average burned area for the first decade in large non-forest wildfires (figures 1 and 2). Unlike the case of forest wildfires where the rightward shift in fire size distribution was most pronounced in the 1980s, rightward shifts in large non-forest wildfire size distribution have been relatively gradual across the last three decades (figure 2).

A similar analysis with shorter duration BLM fire records produced comparable results. While there was no statistically significant change in the frequency of large BLM fires in non-forest vegetation ($p = 0.73$), there was a statistically significant increase in the frequency of large BLM forest fires ($p = 0.007$). Increases in burned area in large BLM forest fires were highly significant ($p = 0.007$), and increases in burned area in BLM non-forest wildfires were also significant ($p = 0.04$). Percentage increases showed the same pattern as USFS, BIA and NPS fires, with percentage increases in forest wildfires' burned area much larger than for non-forest wildfires.

Table 3. Fire season length and fire burn time by decade.^a

| | 1973 – 1982 | 1983 – 1992 | 1993 – 2002 | 2003 – 2012 |
|--------------------|-------------|-------------|-------------|-------------|
| five forest areas | | | | |
| first discovery | 154 | 150 | 115 | 120 |
| last discovery | 284 | 286 | 281 | 282 |
| last control | 292 | 316 | 316 | 342 |
| season length | 138 | 166 | 202 | 222 |
| mean burn time | 6 | 23 | 40 | 52 |
| years with no fire | 0 | 1 | 0 | 0 |
| Northern Rockies | | | | |
| first discovery | 210 | 190 | 196 | 183 |
| last discovery | 250 | 260 | 256 | 263 |
| last control | 258 | 298 | 310 | 317 |
| season length | 49 | 107 | 114 | 134 |
| mean burn time | 7 | 27 | 48 | 59 |
| years with no fire | 1 | 1 | 2 | 0 |
| Northwest | | | | |
| first discovery | 206 | 211 | 203 | 298 |
| last discovery | 223 | 243 | 234 | 252 |
| last control | 229 | 254 | 287 | 315 |
| season length | 23 | 43 | 84 | 116 |
| mean burn time | 7 | 13 | 41 | 54 |
| years with no fire | 5 | 2 | 3 | 1 |
| Sierra Nevada | | | | |
| first discovery | 183 | 193 | 185 | 183 |
| last discovery | 241 | 256 | 269 | 268 |
| last control | 248 | 274 | 294 | 323 |
| season length | 65 | 81 | 109 | 140 |
| mean burn time | 8 | 17 | 27 | 49 |
| years with no fire | 2 | 1 | 1 | 0 |
| Southwest | | | | |
| first discovery | 177 | 152 | 115 | 125 |
| last discovery | 243 | 220 | 248 | 250 |
| last control | 249 | 246 | 282 | 307 |
| season length | 72 | 94 | 167 | 182 |
| mean burn time | 3 | 20 | 37 | 41 |
| years with no fire | 2 | 1 | 1 | 0 |
| Southern Rockies | | | | |
| first discovery | 183 | 175 | 165 | 169 |
| last discovery | 209 | 219 | 231 | 232 |
| last control | 214 | 227 | 263 | 286 |
| season length | 31 | 52 | 98 | 117 |
| mean burn time | 5 | 10 | 27 | 37 |
| years with no fire | 3 | 6 | 2 | 0 |

^aRounded to the nearest whole day, excluding years with no large fires.

Most of the increase in large wildfires is due to lightning-ignited wildfires (figure 1). Less than 12% of the trend in large forest fires on USFS, NPS and BIA lands is

due to changes in human-ignited wildfires. For non-forest fires, there was no significant trend at all in human-caused fires.

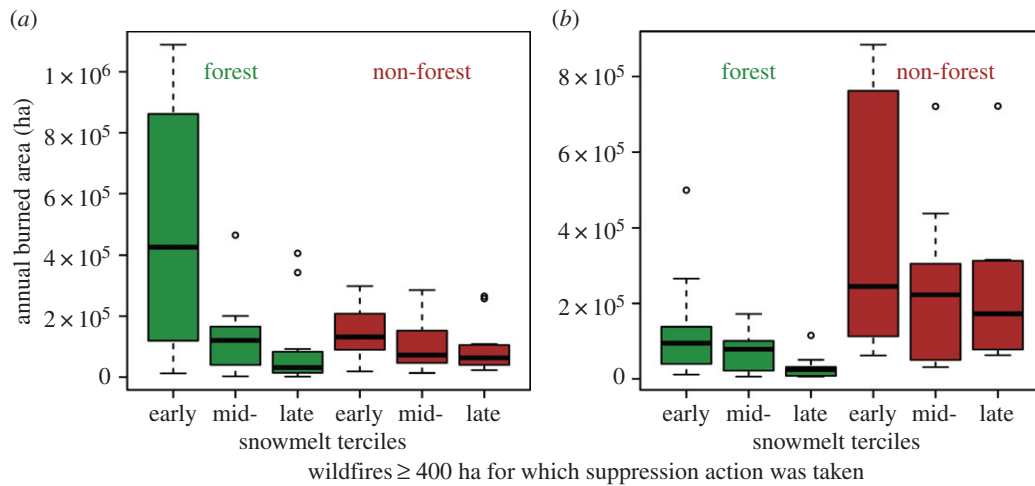


Figure 4. Annual burned area by coarse vegetation type and snowmelt tercile for USFS, NPS and BIA wildfires (1973–2012) (a), and BLM wildfires (1980–2012) (b).

(b) Forest wildfire, temperature and the timing of spring snowmelt

Annual large forest wildfire frequency in USFS, NPS and BIA forests is significantly correlated with spring and summer temperature (Spearman's rank correlation $\rho > 0.7$; figure 3). The largest fires years occur in years with warm spring and summer temperatures and early spring snowmelt dates.

Fire seasons in 2003–2012 averaged more than 84 days longer than in 1973–1982, reflecting a positive trend of just over three days per year since the 1970s (figure 3, table 3). While first discovery dates were over two weeks later on average in 2003–2012 compared with 1993–2002, later control dates more than compensated. This reflects the fact that over the last four decades, the average large wildfire burn time grew from nearly six days in 1973–1982, to nearly 20 days in 1983–1992, nearly 37 days in 1993–2002 and over 50 days in 2003–2012 (table 3).

The earliest third of spring snowmelt years accounts for more than 70% of the area burned in large forest wildfires, and 43% of the area burned in non-forest fires, in the 1970–2012 USFS, NPS and BIA record (figure 4). Early-tercile snowmelt years account for 57% and 50%, respectively, of the burned area for forest and non-forest wildfires in the shorter 1980–2012 BLM record (figure 4). Kruskal–Wallis tests for stochastic dominance were highly significant in each case, indicating that the distribution of at least one tercile deviated significantly from the other two. Dunn's tests indicated that the early- and late-tercile burned areas were significantly different for both forest and non-forest fires in the combined USFS, NPS and BIA fire history, as well as for the forest fires in the BLM fire history. However, the test could not reject the null hypothesis of no difference between early- and late-tercile non-forest BLM wildfire annual burned area. This may be due to the shorter time series available for BLM wildfires, which differentially reduced the sample of late-tercile wildfires more than for early-tercile wildfires, since the terciles were defined for the full 1970–2012 period. The BLM data do confirm, however, the significant effect of spring snowmelt timing on forest wildfire.

(c) Drivers of forest wildfire sensitivity to timing of spring

While the frequency of large forest wildfires regionally is sensitive to timing of spring snowmelt driven by warming

temperatures, analysis of the effects of spring snowmelt timing within western US forests revealed highly diverse responses of forest wildfire. Forests with historic mean snow-free periods of approximately two to four months and high cumulative spring and summer AET have been most sensitive to changes in moisture deficit associated with spring timing (figure 5). Mid-elevation forests in the US Rocky Mountains and the Sierra Nevada have had the largest forest areas with the most drying associated with early spring snowmelt timing compared with late spring snowmelt timing. These areas also show the greatest increases in large-fire frequency from early to late snowmelt seasons (figure 5). The best fit functional form for large forest wildfire frequency response to snowmelt timing was exponential: ($p < 2 \times 10^{-16}$, $R^2 = 0.91$). That is, more than 90% of the spatial variability in the shift in large wildfire frequency between early and late snowmelt years was explained by an exponential function of the change in forest-area weighted moisture deficit.

Note that while SW forests had highly significant trends in large fires and burned area (tables 1 and 2), dry years there with increased fire activity were not significantly associated with the index of spring snowmelt timing (CT1) used here. Unlike Rocky Mountain forests, the largest SW forest fires occurred in both early and late spring snowmelt years. The streamflow CT record is dominated by stations further north in the Rocky Mountains, whereas climate in the Southwest can diverge markedly from the Northwest. For example, 2011 was warm and dry in the Southwest and coincided with an extreme fire season there, but 2011 was a late spring snowmelt year as reflected in CT1, with a north–south climate dipole pattern consistent with a strong La Niña event [28,29].

4. Discussion

Previous studies have suggested forest wildfire activity in the western US is increasing due to a warming climate and earlier spring snowmelt, with Northern Rocky Mountain forests particularly sensitive to these changes [1,2,5,6]. Here, we see that wildfire frequency and burned area in Pacific Northwest forests have increased more rapidly, albeit from a low base, in the most recent two decades (tables 1 and 2). Wildfire

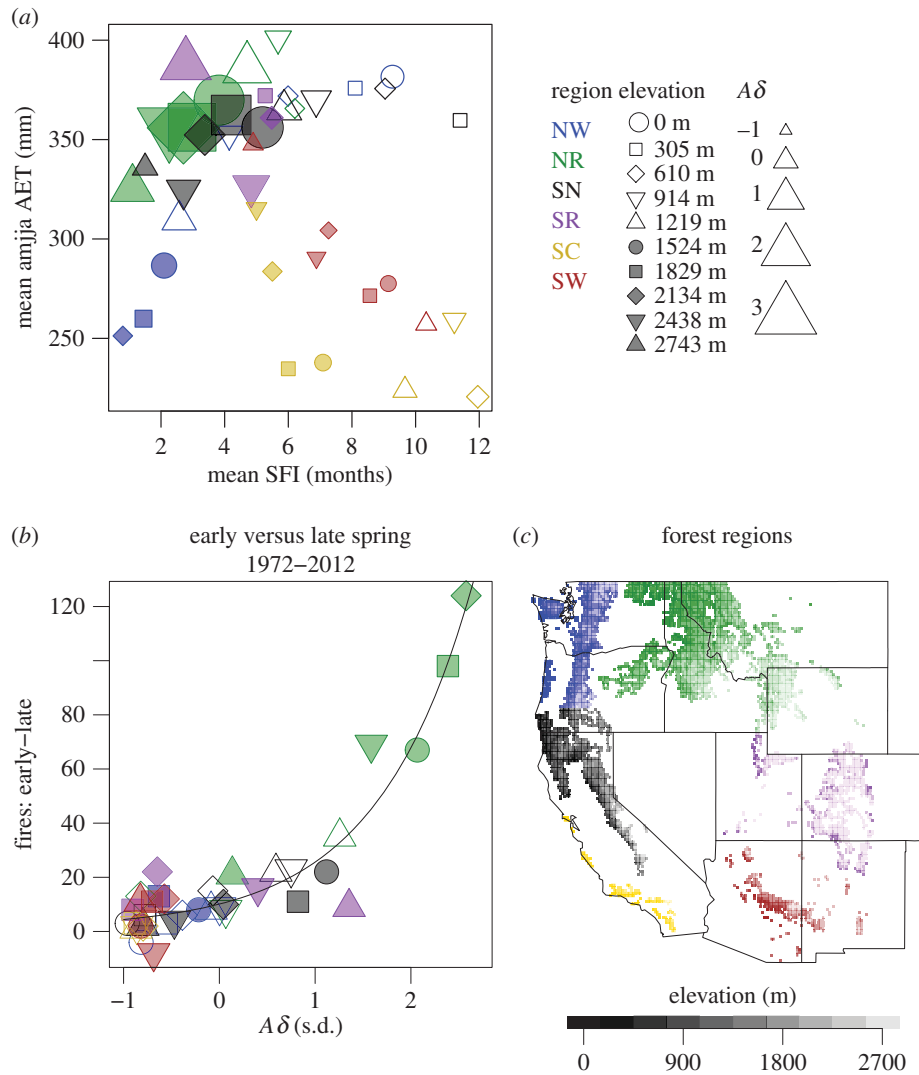


Figure 5. (a) Standardized per cent change in forest-area weighted moisture deficit ($A\delta$) from early versus late snowmelt years by forest area and elevation plotted against mean snow-free season and April–August AET; legend: point colour indicates forest area, shape indicates elevation in 300 m bands and size indicates $A\delta$ in standard deviations; (b) scatter plot of early snowmelt year minus late snowmelt year wildfires versus $A\delta$ with regression fit to $\exp(A\delta)$ (line); (c) map of western US forest area: shading indicates elevation, colour indicates forest region.

activity in other vegetation types may also be increasing (figure 1), and at least for some federally managed lands that increase is strongly associated with the timing of spring snowmelt (figure 4).

Within western US forest areas there is great diversity in the response of wildfire activity to changes in the timing of spring. The most sensitive forests are ones that historically had a mean snow-free season of just two to four months, and high spring and summer cumulative AET. A forest-area weighted moisture deficit index ($A\delta$) that integrates both the intensity of drying and the forest area affected by drying due to shifts in the timing of spring explains most of the spatial variability in changes in large forest wildfire frequency associated with early versus late spring snowmelt. Increases in fire frequency scale exponentially with changes in cumulative water-year deficit ($A\delta$). Given projections for further drying within the region due to human-induced warming, this study underlines the potential for further increases in wildfire activity [7,13,14].

Atmospheric circulation patterns have a broad regional footprint that produces high spatial correlation in temperature anomalies. Thus, early spring snowmelt years still imply warm, early springs in locations that receive little or

no snow. While greater AET in early months may extend the length of the summer drought, locations where AET in the dry season is more constrained by available moisture may not see as much change in cumulative moisture deficit over the full seasonal cycle (figure 5). Thus, sensitivity of large wildfire frequency to timing of spring is greatest in forests where snow is a significant portion of annual precipitation and moisture availability is less of a constraint on AET.

Increasing population and development in proximity to fire-prone lands are sometimes called out as potential drivers of increased wildfire activity. However, the very small contribution of human-caused ignitions to trends in wildfire (figure 1) seems to indicate that these do not play an important role in driving changes in western US wildfire.

Strong trends in Southwestern wildfire that do not appear to be associated with changes in the regional timing of spring index may lend support to the observations and argument that human-induced changes in forest composition, density and structure are particularly important to changes in wildfire in Southwestern forests [30]. At the same time, the start of the Southwestern fire season—as indicated by the date of first large-fire discovery—has shifted more than 50 days earlier since the 1970s, accounting for about one-third of the

increase in the length of the fire season there (table 3). The substantially earlier SW fire season start is consistent with warmer temperatures and earlier spring seasons leading to earlier flammability of fuels in SW forests. However, the spring snowmelt timing index used here (CT1) is dominated by observations recorded in Northern and Central US Rocky Mountain streams, and may not be consistently representative of the timing of spring snowmelt in Southwestern mountain forests.

Changing fire suppression tactics are frequently posited to have contributed to changes in wildfire activity in recent decades. While wildfires used in this analysis were recorded as actively suppressed ‘action’ fires, that does not rule out changing tactics over time altering the effectiveness of suppression and, consequently, the distribution of large

wildfire sizes. Western US wildfire is a coupled human and natural system, and it is reasonable to anticipate that the profound changes observed in climate and wildfire activity over recent decades could elicit changes in wildfire and land management practices that feed back into subsequent wildfire activity, shaping ecosystem sensitivity to further climatic change.

Competing interests. I have no competing interests.

Funding. This research was supported by the California Nevada Applications Program under NOAA grant no. NA110AR4310150.

Acknowledgements. I thank Jeanne Milostan and Alisa Keyser for their assistance during the course of this project, the reviewers for their constructive comments and the editors for their patience. Any errors or omissions are my own.

References

- Westerling AL, Hidalgo HG, Cayan DR, Swetnam TW. 2006 Warming and earlier spring increase western US forest wildfire activity. *Science* **313**, 940–943. (doi:10.1126/science.1128834)
- Morgan P, Heyerdahl EK, Gibson CE. 2008 Multi-season climate synchronized forest fires throughout the 20th century, northern Rockies, USA. *Ecology* **89**, 717–728. (doi:10.1890/06-2049.1)
- Littell JS, McKenzie D, Peterson DL, Westerling AL. 2009 Climate and wildfire area burned in western US ecoprovinces, 1916–2003. *Ecol. Appl.* **19**, 1003–1021. (doi:10.1890/07-1183.1)
- Westerling AL, Turner MG, Smithwick EA, Romme WH, Ryan MG. 2011 Continued warming could transform Greater Yellowstone fire regimes by mid-21st century. *Proc. Natl Acad. Sci. USA* **108**, 13 165–13 170. (doi:10.1073/pnas.1110199108)
- Kitzberger T, Brown PM, Heyerdahl EK, Swetnam TW, Veblen TT. 2007 Contingent Pacific–Atlantic Ocean influence on multicentury wildfire synchrony over western North America. *Proc. Natl Acad. Sci. USA* **104**, 543–548. (doi:10.1073/pnas.0606078104)
- Heyerdahl EK, Morgan P, Riser JP. 2008 Multi-season climate synchronized historical fires in dry forests (1650–1900), northern Rockies, USA. *Ecology* **89**, 705–716. (doi:10.1890/06-2047.1)
- Williams AP *et al.* 2013 Temperature as a potent driver of regional forest drought stress and tree mortality. *Nat. Clim. Change* **3**, 292–297. (doi:10.1038/nclimate1693)
- Flannigan MD, Krawchuk MA, de Groot WJ, Wotton BM, Gowman LM. 2009 Implications of changing climate for global wildland fire. *Int. J. Wildland Fire* **18**, 483–507. (doi:10.1071/WF08187)
- Krawchuk MA, Moritz MA. 2011 Constraints on global fire activity vary across a resource gradient. *Ecology* **92**, 121–132. (doi:10.1890/09-1843.1)
- Westerling AL, Gershunov A, Brown TJ, Cayan DR, Dettinger MD. 2003 Climate and wildfire in the western United States. *Bull. Am. Meteorol. Soc.* **84**, 595. (doi:10.1175/BAMS-84-5-595)
- Turner MG. 2010 Disturbance and landscape dynamics in a changing world 1. *Ecology* **91**, 2833–2849. (doi:10.1890/10-0097.1)
- Osmond CB, Pitelka LF, Hidy GM (eds). 2012 *Plant biology of the basin and range*. Berlin, Germany: Springer Science & Business Media.
- Seager R *et al.* 2007 Model projections of an imminent transition to a more arid climate in southwestern North America. *Science* **316**, 1181–1184. (doi:10.1126/science.1139601)
- Barnett TP *et al.* 2008 Human-induced changes in the hydrology of the western United States. *Science* **319**, 1080–1083. (doi:10.1126/science.1152538)
- Mitchell KE *et al.* 2007 The multi-institution North American land data assimilation system (NLDAS): utilizing multiple GCM products and partners in a continental distributed hydrological modeling system. *J. Geophys. Res.* **109**, D07S90. (doi:10.1029/2003JD003823)
- Wood AW, Lettenmaier DP. 2006 A test bed for new seasonal hydrologic forecasting approaches in the western United States. *Bull. Am. Meteorol. Soc.* **87**, 1699. (doi:10.1175/BAMS-87-12-1699)
- Liang X, Lettenmaier DP, Wood EF, Burges SJ. 1994 A simple hydrologically based model of land surface water and energy fluxes for general circulation models. *J. Geophys. Res.* **99**, 14 415–14 428. (doi:10.1029/94JD00483)
- Penman HL. 1948 Natural evaporation from open water, bare soil and grass. *Proc. R. Soc. Lond. A*, **193**, 120–145. (doi:10.1098/rspa.1948.0037)
- Monteith JL. 1965 Evaporation and environment. *Symp. Soc. Expl. Biol.* **19**, 205–234.
- Coles S. 2001 *An introduction to statistical modeling of extreme values*. London, UK: Springer.
- Bauer DF. 1972 Constructing confidence sets using rank statistics. *J. Am. Stat. Assoc.* **67**, 687–690. (doi:10.1080/01621459.1972.10481279)
- NCDC. 1994 Time bias corrected divisional temperature-precipitation-drought index. (Documentation for dataset TD-9640. Available from DBMB, NCDC, NOAA, Federal Building, 37 Battery Park Ave. Asheville, NC 28801-2733).
- Stewart IT, Cayan DR, Dettinger MD. 2005 Changes toward earlier streamflow timing across western North America. *J. Clim.* **18**, 1136–1155. (doi:10.1175/JCLI3321.1)
- Cayan DR, Dettinger MD, Kammerdiener SA, Caprio JM, Peterson DH. 2001 Changes in the onset of Spring in the western United States. *Bull. Am. Meteorol. Soc.* **82**, 399–415. (doi:10.1175/1520-0477(2001)082<0399:CIT00S>2.3.CO;2)
- Slack JR, Landwehr JM. 1992 *US Geological Survey open-file report 92–129: Hydro-Climatic Data Network: a US Geological Survey Streamflow Data Set for the United States for the Study of Climatic Variations: 1874–1988*. Reston, VA: US Geological Survey.
- Dunn OJ. 1964 Multiple comparisons using rank sums. *Technometrics* **6**, 241–252. (doi:10.1080/00401706.1964.10490181)
- Burnham KP, Anderson DR. 2003 *Model selection and multimodel inference: a practical information-theoretic approach*. Berlin, Germany: Springer Science & Business Media.
- Swetnam TW, Brown PM. 2011 Climatic inferences from dendroecological reconstructions. In *Dendroclimatology*, pp. 263–295. Dordrecht, The Netherlands: Springer.
- Hurteau MD, Bradford JB, Fulé PZ, Taylor AH, Martin KL. 2014 Climate change, fire management, and ecological services in the southwestern US. *For. Ecol. Manage.* **327**, 280–289. (doi:10.1016/j.foreco.2013.08.007)
- Allen CD *et al.* 2002 Ecological restoration of Southwestern ponderosa pine ecosystems: a broad perspective. *Ecol. Appl.* **12**, 1418–1433. (doi:10.1890/1051-0761(2002)012[1418:EROSPP]2.0.CO;2)